

MORPHOLOGICAL AND INTERLAYER GEOCHEMICAL STUDIES ON MANGANESE NODULES FROM THE SOUTHWESTERN CARLSBERG RIDGE

A.B. VALSANGKAR, G.V. RAJAMANICKAM*, S.M. KARISIDDAIAH and H.N. SIDDIQUIE⁺

National Institute of Oceanography, Dona Paula, Goa 403004 (India)

(Received November 23, 1987, revised and accepted June 6, 1988)

Abstract

Valsangkar, A.B., Rajamanickam, G.V., Karisiddaiah, S.M. and Siddiquie, H.N., 1988. Morphological and interlayer geochemical studies on manganese nodules from the southwestern Carlsberg Ridge. *Mar. Geol.*, 84: 81–94.

Mixed facies of manganese nodules from the southwestern Carlsberg Ridge have been analysed for Mn, Fe, Ni, Cu, Co and Zn. We present 71 analyses including the averages for outer layer, inner layer and near-core material. Morphological studies show seven types of nodules of which medium-size spheroidal, ellipsoidal and intergrown nodules are most abundant. Only spheroidal and ellipsoidal nodules with rough surfaces show higher concentrations of Mn, Fe, Cu, Ni, Co and Zn towards the outer layer, whereas the smooth-surface nodules other than the spheroidal type show higher concentrations of these elements towards the core region. The other nodule types show a decreasing content of these elements in all the layers analysed. Copper and Ni are present in low concentrations and are associated with Zn and Mn. The mineralogy indicates diagenetic processes involving metal remobilisation, and the chemistry suggests the precipitation of metals mostly from seawater. Variations in the source of supply of the elements are responsible for the observed variations in the chemical composition of the nodules.

Introduction

Manganese nodules from the Carlsberg Ridge have previously been studied by Cronan (1967), Cronan and Tooms (1968), Glasby (1970, 1972, 1973), Dunham and Glasby (1974), Colley et al. (1979) and Cronan and Moorby (1981). As a part of the exploration for marine minerals, manganese nodules were collected from nine locations on the southwestern flank of the Carlsberg Ridge (Fig.1) during the 1981 cruises of R.V. *Gaveshani*.

The depth in the sampling area varies from 3900 to 4500 m and the 3.5 kHz profiles across

the Carlsberg Ridge show a rugged topography of ridges and valleys. The profiles show a weakly reflecting sediment with a maximum thickness of about 60 m on the southwestern flank of the ridge. The sediment samples comprise white to dark brown calcareous oozes. Foraminiferal oozes commonly occur on the topographic highs above 3500 m whereas siliceous oozes are found in the valleys. Surficial deposits of manganese nodules occur on the slopes of the ridges.

Methods

Sampling techniques

Samples of manganese nodules and sediments were collected with a Petterson grab

*Present address: Department of Ancient Industries, Tamil University, Thanjavur 613001 (India).

⁺Deceased.

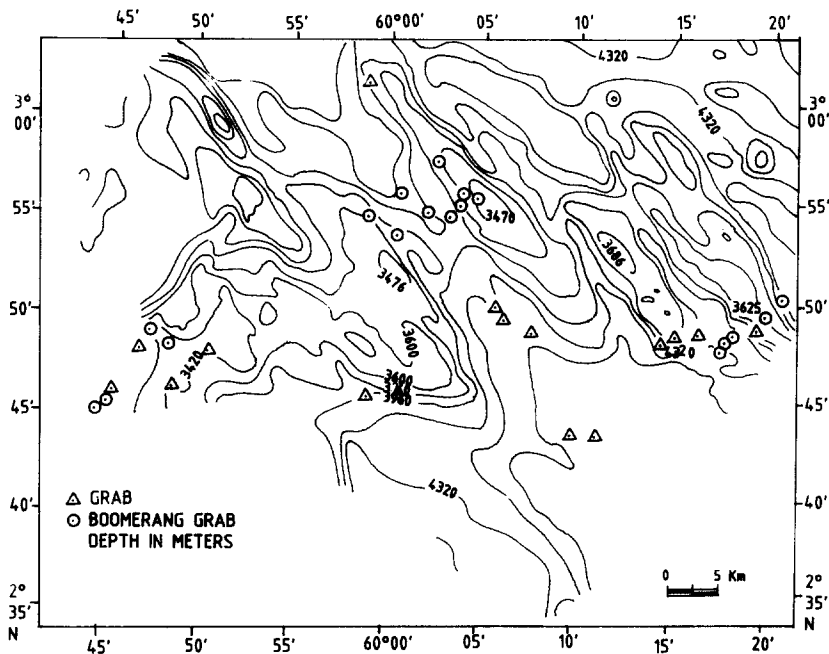


Fig.1. Bathymetry and locations of sampling stations.

with a triggering mechanism and by free-fall grabs. The nodule abundance (kg/m^2) was estimated by weighing, and after initial on-board classification based on surface texture and diameter using Meyer's (1973) scheme, the classification was revised in the laboratory using the scheme of Moritani et al. (1977). The nodules were then measured for minimum and maximum diameter and compared with standard weights and compositions. A medium-size nodule was selected from each size class for chemical analysis.

Analytical techniques

The nodule samples were washed free of salt and sediment and split into layers with a steel splitter. These layers are designated as outermost layer (OL), inner intermediate layer (IL) and near-core layer (Core). A typical nodule with the various layers is shown in Fig.2. In carrying out layer-by-layer analyses, the nucleus was not included. The term "Core" (capitalised) used from here on indicates material with the nucleus not included.

The samples were ground in an agate mortar

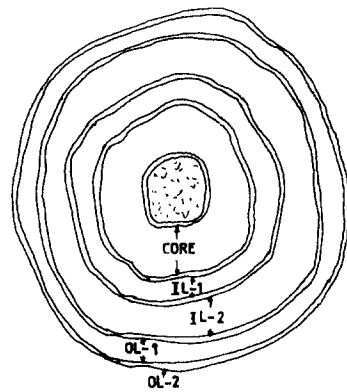


Fig.2. The various analysed layers.

and dried for 36 h in an oven at constant temperature (110°C). A sample of 0.1 g of powder in a platinum crucible was dissolved using HF, HNO_3 and HClO_4 . The final solutions were made by adding 10% boric acid. The solutions were analysed on a Model 5000 Perkin-Elmer atomic absorption spectrophotometer for Mn, Fe, Ni, Cu, Co and Zn. The texture and mineralogy of the nodules was studied with the use of thin and polished sections, SEM and a Philips X-ray Diffracto-

meter (XRD) with an Fe-K α and manganese filter.

Results

Size, abundance and texture

Seven different types of nodules were identified and their physical properties and size parameters are listed in Table 1. The average concentrations of Mn, Fe, Ni, Cu, Co and Zn are plotted against the maximum diameter (Fig.3). With increasing diameter, Mn, Cu and Co increase whereas Fe and Zn decrease. Nickel shows no significant variation.

Within the sampling area, the population density of smooth-surface nodules is greater than that of rough-surface nodules. The abundance of nodules in the sample area varies from 1.1 to 5.8 kg/m² (Table 1). The nodule cores consist of weathered rock fragments and occasional hard clay relicts.

Mineralogy

X-ray diffraction studies showed that the mineral phases are not well crystallised. In a

few samples, diffuse peaks of todorokite were observed. However, none of the samples clearly showed a well-crystallised todorokite peak. The common mineral phase in the nodules is δ -MnO₂.

Polished sections show columnar, mottled and microlaminated textures and SEM examination of selected samples shows alternate layers of δ -MnO₂ and FeOOH.XH₂O sometimes associated with todorokite. SEM studies revealed that todorokite occurs in interstitial spaces and as secondary infillings or as veinlets. Occasionally, it also occurs as pods and in interstitial spaces associated with agglutinated foraminifera. The thin sections are opaque and therefore no significant features could be detected. Altered basalt fragments, olivine pseudomorphs and occasionally volcanic glass, clay and fragments of other nodules are seen in the nuclei. More detailed studies on the mineralogy of these nodules has been carried out by Karisiddaiah (1985).

Composition

Fifty-three analyses of eighteen specimens from nine stations are presented (Table 1, Fig.4). Two-three analyses of each specimen

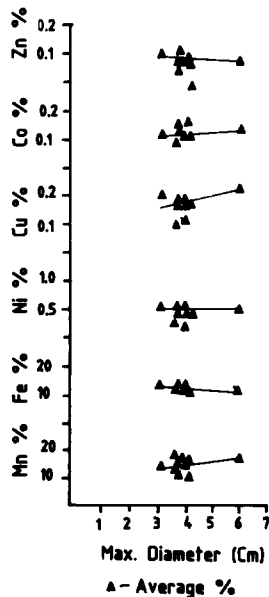


Fig. 3. Comparison between the average Mn, Fe, Ni, Cu, Co and Zn content and the maximum diameter of the nodules.

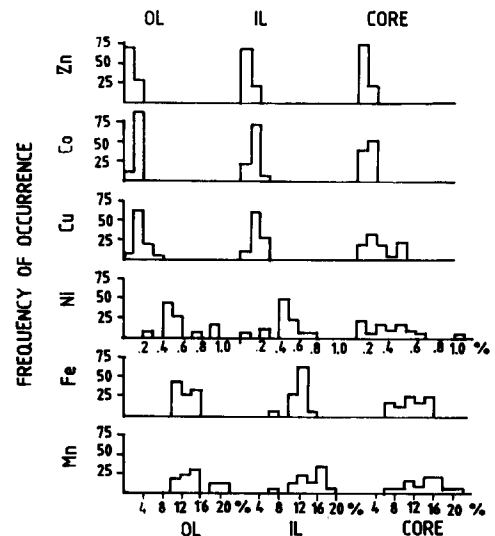


Fig.4. Frequency distribution of Mn, Fe, Ni, Cu, Co and Zn in layers OL, IL and Core.

TABLE 1
Major element concentration of manganese nodules from the Carlsberg Ridge

No.	Station No.	Average depth (m)	Lat. (°N)	Long. (°E)	Abundance kg/m ²	Nodule type	Maximum diameter (cm)	Layer	Mn (%)	Fe (%)	Ni (%)	Cu (%)	Co (%)	Zn (%)	Mn/Fe	Cu/Ni	Ni+Cu (%)	Ni+Cu+Co (%)
1	1902	4400	2 45.8	59 59.0	2.16	Ss	3.7	OL	11.75	13.00	0.45	0.15	0.13	0.05	0.90	0.33	0.60	0.73
2								IL	7.50	12.10	0.28	0.09	0.06	0.05	0.62	0.32	0.37	0.43
3								Core	19.00	10.20	0.15	0.05	0.07	0.04	1.86	0.33	0.20	0.27
4								Av	12.75	11.77	0.29	0.10	0.09	0.05	1.13	0.34	0.39	0.48
5	1907/1	4500	2 55.2	60 2.3	5.85	ISs	4.2	OL-1	14.65	12.22	0.43	0.18	0.14	0.08	1.20	0.42	0.61	0.75
6								OL-2	14.75	12.20	0.62	0.19	0.13	0.09	1.23	0.31	0.81	0.94
7								IL	13.00	12.40	0.46	0.22	0.22	0.08	1.05	0.48	0.68	0.75
8								Core	10.90	6.60	0.21	0.08	0.68	0.04	1.65	0.38	0.29	0.97
9								Av	13.33	10.80	0.43	0.17	0.29	0.07	1.28	0.40	0.60	0.86
10	1908/3	4320	2 55.0	59 58.4	2.36	DPs	3.8	OL	20.75	11.50	0.92	0.33	0.16	0.09	1.80	0.36	1.25	1.41
11								IL	11.50	13.40	0.51	0.16	0.14	0.07	0.86	0.31	0.66	0.88
12								Core	10.25	14.70	0.42	0.15	0.16	0.05	0.70	0.36	0.57	0.73
13								Av	11.66	12.93	0.56	0.17	0.15	0.08	0.90	0.31	0.73	0.88
14	1925	4000	1 18.8	58 43.1	1.10	Sr	6.0	OL	20.75	11.50	0.92	0.33	0.16	0.09	1.80	0.36	1.25	1.41
15								IL-1	17.50	10.80	0.49	0.20	0.13	0.08	1.62	0.41	0.69	0.82
16								IL-2	13.75	12.70	0.10	0.20	0.13	0.07	1.08	0.20	0.30	0.43
17								Core	16.75	11.50	0.56	0.20	0.14	0.07	1.46	0.36	0.76	0.90
18								Av	17.19	11.62	0.52	0.23	0.14	0.08	1.48	0.44	0.75	0.89
19	1932	4000	2 56.6	60 5.2	4.53	Db	4.1	OL	18.75	10.50	0.53	0.26	0.14	0.10	1.79	0.49	0.79	1.03
20								IL	14.00	14.00	0.40	0.11	0.16	0.07	1.00	0.28	0.51	0.67
21								Core	14.50	12.30	0.35	0.14	0.17	0.06	1.18	0.40	0.49	0.66
22								Av	15.75	12.27	0.43	0.17	0.16	0.08	1.28	0.40	0.60	0.76
23								OL	15.25	12.80	0.54	0.20	0.13	0.05	1.19	0.37	0.74	0.87
24								IL	13.25	14.00	0.41	0.15	0.09	0.04	0.95	0.37	0.56	0.65
25								Core	11.75	14.80	0.39	0.21	0.14	0.07	0.79	0.54	0.60	0.74
26								Av	13.42	13.87	0.45	0.19	0.12	0.05	0.97	0.42	0.64	0.76
27								OL	19.25	13.40	0.51	0.16	0.14	0.08	1.44	0.31	0.67	0.81
28								IL	17.50	11.20	0.60	0.16	0.07	0.07	1.56	0.27	0.76	0.83
29								Core	16.75	10.10	0.67	0.24	0.15	0.09	1.66	0.36	0.91	1.06
30								Av	17.83	11.57	0.59	0.19	0.12	0.08	1.54	0.32	0.78	0.90
31								OL	10.50	12.00	0.44	0.16	0.14	0.09	1.14	0.50	0.71	0.76
32								IL	16.75	14.70	0.50	0.21	0.05	0.09	1.14	0.50	0.71	0.76
33								Core	21.00	9.20	1.10	0.34	0.10	0.10	2.28	0.31	1.44	1.54
34								Av	16.08	11.97	0.68	0.28	0.10	0.09	1.34	0.35	0.92	1.02
35								OL	16.00	12.27	0.49	0.17	0.13	0.08	1.26	0.35	0.66	0.79
36								IL	13.00	13.30	0.48	0.17	0.12	0.07	0.98	0.35	0.65	0.77
37								Core	13.25	9.40	0.77	0.26	0.13	0.09	1.41	0.34	1.03	1.16
38								Av	14.08	11.80	0.58	0.20	0.13	0.08	1.19	0.34	0.78	0.91
39								OL	4.00	11.20	0.45	0.15	0.13	0.09	1.25	0.33	0.60	0.73

40						Core	13.25	7.10	0.59	0.27	0.10	0.08	1.87	0.46	0.86	0.96
41						Av	13.63	9.15	0.52	0.21	0.12	0.09	1.49	0.40	0.73	0.85
42						OL	13.50	12.00	0.52	0.19	0.13	0.08	1.13	0.37	0.71	0.84
43					SPr	3.1	11.00	12.60	0.49	0.22	0.14	0.08	0.87	0.49	0.71	0.85
44						Core	15.50	10.40	0.66	0.42	0.11	0.12	1.49	0.64	1.08	1.19
45						Av	13.33	11.67	0.56	0.28	0.13	0.09	1.14	0.50	0.84	0.97
46					SPs	3.4	18.00	11.40	0.63	0.27	0.11	0.14	1.58	0.43	0.90	1.01
47						Core	17.25	14.20	0.53	0.16	0.11	0.13	1.21	0.30	0.69	0.80
48						Av	17.63	12.80	0.58	0.22	0.11	0.14	1.38	0.38	0.80	0.91
49					Sr	3.5	14.00	14.30	0.42	0.15	0.11	0.12	0.98	0.36	0.57	0.68
50						Core	10.00	10.90	0.39	0.19	0.11	0.12	0.91	0.49	0.58	0.69
51						Av	12.00	12.60	0.41	0.17	0.11	0.12	0.95	0.41	0.58	0.69
52					Sr	3.5	14.00	14.30	0.58	0.26	0.11	0.12	0.98	0.49	0.84	0.95
53						IL	10.25	12.40	0.54	0.20	0.17	0.13	0.83	0.37	0.74	0.91
54						Core	6.77	12.50	0.13	0.07	0.04	0.10	0.54	0.54	0.20	0.24
55						Av	10.31	13.07	0.42	0.18	0.11	0.12	0.79	0.43	0.60	0.71
56	1934	•	3900	2 46.3	59 47.5	SPs	15.25	13.60	0.41	0.15	0.14	0.07	1.12	0.37	0.56	0.70
57						OL-1										
58						IL	11.75	13.40	0.45	0.20	0.10	0.13	0.88	0.44	0.65	0.75
59						Av	18.00	11.70	0.48	0.16	0.11	0.06	1.54	0.33	0.64	0.75
60						IL	15.00	12.90	0.45	0.17	0.12	0.09	1.16	0.38	0.62	0.74
61					SPs	2.9	15.75	13.10	0.49	0.18	0.13	0.13	1.20	0.37	0.76	0.80
62	1935/1	3900	2 50.6	6 20.1	3.34	ISs	14.75	15.10	0.28	0.10	0.15	0.11	0.98	0.36	0.38	0.53
63						IL	15.75	7.50	0.27	0.08	0.14	0.11	2.10	0.30	0.35	0.49
64						Core	18.25	12.40	0.13	0.19	0.07	0.04	1.47	1.46	0.32	0.39
65						Av	16.25	11.67	0.23	0.12	0.12	0.09	1.39	0.52	0.35	0.47
66	1935/2	4100	2 49.5	60 19.6	3.03	Ss	20.80	10.80	0.94	0.26	0.07	0.09	1.90	0.28	1.20	1.27
67						IL-1	14.25	12.80	0.58	0.20	0.17	0.09	1.11	0.34	0.78	0.95
68						IL-2	19.00	12.00	0.73	0.21	0.14	0.07	1.58	0.29	0.94	1.01
69						Core-1	14.05	7.60	0.12	0.05	0.06	0.02	1.85	0.42	0.17	0.23
70						Core-2	14.75	14.40	0.47	0.18	0.17	0.06	1.02	0.38	0.65	0.82
71						Av	16.51	11.52	0.57	0.18	0.12	0.07	1.43	0.32	0.75	0.87

Layers: *OL* --- outer layer; *IL* --- inner layer; *Av* --- average. Nodule types: *Ss* --- small to medium, smooth surface, spheroidal/ellipsoidal; *ISs* --- large, smooth surface, irregular/flattened; *DPs* --- small to medium, smooth surface, flat/elongated; *Sr* --- small to medium, rough surface, spheroidal/ellipsoidal; *Db* --- medium to large, rough surface, discoidal; *SPs* --- small to medium, smooth surface, intergrown; *SPr* --- small to medium, rough surface, intergrown.

representing OL, IL and Core samples were determined. In this way the variation in particular elements from Core to OL could be studied. Different types of nodules were analysed to ascertain if systematic relationships exist for a given nodule population.

The analyses show that in most cases there are both increases and decreases of individual elements from OL to Core (Table 1). Closer examination shows that from OL to Core the concentrations of Ni, Cu, Co and Zn decrease in Ss-type nodules; Mn, Fe, Ni, Cu, Co and Zn either decrease or increase in ISs, DPs- and SPs-type nodules; Mn, Fe, Ni, Cu, Co, Zn and Mn/Fe typically decrease in Sr-type nodules; Mn, Fe, Ni, Cu, Co and Zn decrease in Db-type

nodules and Mn, Fe, Co and Zn decrease and Ni and Cu increase in SPr-type nodules. Results similar to these are seen in Tables 2A and B and in Fig.4.

The highest concentrations of the elements compared to the nodule type are shown in Table 2A. The averages show interesting results: Mn is highest in SPr-type nodules, Fe in the SPs-type, Ni in the DPs-type, Cu in the DPs-types, Co in the ISs-type, and Zn in the SPs-type nodules. Further, the SPs-type nodules typically show enrichment of Zn in all three layers (OL, IL and Core). Another interesting observation is that out of the seven types of nodules, only three (DPs, SPs and ISs) show highest Core concentrations

TABLE 2A

Occurrence of the highest concentration of the various elements in layers OL, IL and Core. (Values in parentheses indicate sample numbers in Table 1)

Nodule type	No. analyses	Mn (%)	Fe (%)	Ni (%)	Cu (%)	Co (%)	Zn (%)	Mn/Fe
Outer layer (OL)								
Ss	3	20.50 (66)	13.00 (1)	0.94 (66)	0.26 (66)	0.13 (1,66)	0.09 (66,39)	1.90 (66)
ISs	3	14.75 (6,62)	15.10 (62)	0.62 (6)	0.19 (6)	0.15 (62)	0.11 (62)	1.23 (6)
DPs	3	20.75 (10)	12.00 (31)	0.92 (10)	0.33 (10)	0.16 (10)	0.09 (10,31)	1.80 (10)
Sr	3	20.75 (14)	14.30 (49,52)	0.92 (14)	0.33 (14)	0.16 (14)	0.12 (49,52)	1.80 (14)
Db	1	18.75 (19)	10.50 (19)	0.53 (19)	0.26 (19)	0.14 (19)	0.10 (19)	1.79 (19)
SPs	3	15.25 (23,56)	13.60 (56)	0.54 (23)	0.20 (23,57)	0.14 (56)	0.13 (57)	1.19 (23)
SPr	2	19.25 (27)	13.40 (27)	0.52 (42)	0.19 (42)	0.14 (27)	0.08 (27,42)	1.44 (27)
Inner layer (IL)								
Ss	3	19.00 (68)	12.80 (67)	0.73 (68)	0.21 (68)	0.17 (67)	0.09 (68)	1.58 (68)
ISs	2	15.75 (63)	12.40 (7)	0.46 (7)	0.22 (7)	0.22 (7)	0.11 (63)	2.10 (63)
DPs	3	16.75 (32)	14.70 (32)	0.51 (11)	0.21 (32)	0.14 (11)	0.09 (32)	1.14 (32)
Sr	3	17.50 (15)	12.70 (16)	0.54 (53)	0.20 (15,16,63)	0.17 (53)	0.13 (53)	1.62 (15)
Db	1	14.00 (20)	14.00 (20)	0.40 (20)	0.11 (20)	0.16 (20)	0.07 (20)	1.00 (20)
SPs	4	18.00 (46,58)	14.00 (24)	0.63 (46)	0.27 (46)	0.13 (60)	0.14 (46)	1.58 (46)
SPr	2	17.50 (28)	11.20 (28)	0.60 (28)	0.16 (28)	0.14 (43)	0.08 (43)	1.56 (28)

TABLE 2A (continued)

Nodule type	No. analyses	Mn (%)	Fe (%)	Ni (%)	Cu (%)	Co (%)	Zn (%)	Mn/Fe
Core								
Ss	4	19.00 (3)	14.40 (70)	0.59 (40)	0.27 (40)	0.17 (70)	0.08 (40)	1.87 (40)
ISs	2	18.25 (64)	12.40 (64)	0.21 (8)	0.19 (64)	0.68 (8)	0.04 (8,64)	1.65 (8)
DPs	3	21.00 (33)	14.70 (12)	1.10 (33)	0.34 (33)	0.16 (12)	0.10 (33)	2.28 (33)
Sr	3	16.75 (17)	12.50 (54)	0.56 (17)	0.20 (17)	0.14 (17)	0.12 (50)	1.46 (17)
Db	1	14.50 (21)	12.30 (21)	0.35 (21)	0.14 (21)	0.17 (21)	0.06 (21)	1.18 (21)
SPs	2	17.25 (47)	14.80 (25)	0.53 (47)	0.21 (25)	0.14 (25)	0.13 (47)	1.21 (47)
SPr	2	16.75 (29)	10.40 (44)	0.67 (29)	0.42 (44)	0.15 (29)	0.32 (44)	1.66 (44)
Average (Av)								
Ss	3	16.51 (71)	11.77 (4)	0.57 (41)	0.21 (41)	0.12 (41,71)	0.09 (41)	1.49 (41)
ISs	2	16.25 (65)	11.67 (65)	0.43 (9)	0.17 (9)	0.29 (9)	0.10 (65)	1.39 (65)
DPs	3	16.08 (34)	12.93 (13)	0.68 (34)	0.28 (34)	0.15 (13)	0.09 (34)	1.34 (34)
Sr	3	17.19 (18)	12.60 (51)	0.52 (18)	0.23 (18)	0.14 (18)	0.12 (51,55)	1.48 (18)
Db	1	15.75 (22)	12.27 (22)	0.43 (22)	0.17 (22)	0.16 (22)	0.08 (22)	1.28 (22)
SPs	4	17.63 (48)	13.87 (26)	0.58 (48)	0.22 (48)	0.13 (61)	0.14 (48)	1.38 (48)
SPr	2	17.83 (30)	11.67 (45)	0.59 (30)	0.28 (45)	0.13 (45)	0.09 (45)	1.54 (30)

For explanation of abbreviations, see Table 1.

TABLE 2B

Nodule types classified according to the highest concentrations of elements with respect to the various layers

Layer	Mn	Fe	Ni	Cu	Co	Zn	Mn/Fe	Nodule types	No. analyses
OL	DPs,Sr	ISs	Ss	DPs,Sr	DPs,Sr	SPs	Ss	5	18
IL	Ss	DPs	Ss	SPs	ISs	SPs	ISs	4	18
Core	DPs	SPs	DPs	SPs	ISs	SPs	DPs	3	17
Av	SPr	SPs	SPr	DPs,SPs	ISs	SPs	SPr	4	18

For explanation of abbreviations, see Table 1.

of, respectively, Mn and Ni; Fe, Cu and Zn; and Co. In the OL, five types (DPs, Sr, ISs, Ss and SPs) show the highest concentrations, respectively, being of Mn, Cu and Co (in the DPs- and Sr-types), Co, Fe and Ni, and Zn (Table 2B). All

these layers (OL, IL and Core) in the smooth-surface nodules (in this case, Ss, ISs- and DPs-types) show characteristically higher Mn/Fe values.

The average chemical compositions of the

analysed nodules from the Carlsberg Ridge are given in Table 3. Compared to the averages reported by Cronan and Moorby (1981) (Table 4), these nodules are lower in Mn, Fe, Cu and Co and higher in Zn and Mn/Fe. The Ni values are similar to those of Cronan and Moorby (1981) and S.I.O. (1982). Further comparisons, with the Indian Ocean averages (Table 4) show that our analyses of the Carlsberg Ridge nodules indicate similar concentrations of Ni, Cu, Zn and similar Mn/Fe ratios, whereas Mn (14.79%), Fe (12.14%), Co (0.15%), Cu/Ni (0.38%) and Ni + Cu + Co (0.76%) are lower. Except for station 1908/3 (Table 3), all samples show Mn/Fe ratios greater than one. The highest Mn/Fe value (1.48) is from station 1925.

In Table 5, the average compositions of

nodules of various morphologies from dredge station 1933 are shown. Comparison between the different nodule types shows that Mn, Fe, Ni, Cu and Zn demonstrate considerable variation, while the variation of Co is negligible.

It can be seen from Figs.5A–D that with an increase in Mn there is an increase in Ni and Cu and a slight increase in Fe. This holds true for all three layers (OL, IL and Core). Cobalt and Zn do not show variation in the OL and IL but in the Core both decrease with an increase in Mn. The average levels of Fe, Co and Zn show no variation when compared to Mn, however, there is a slight increase in Cu and Ni with an increase in Mn (Fig.5D).

Copper and Ni show a strong positive correlation in the OL, IL and Core (Fig.6) and

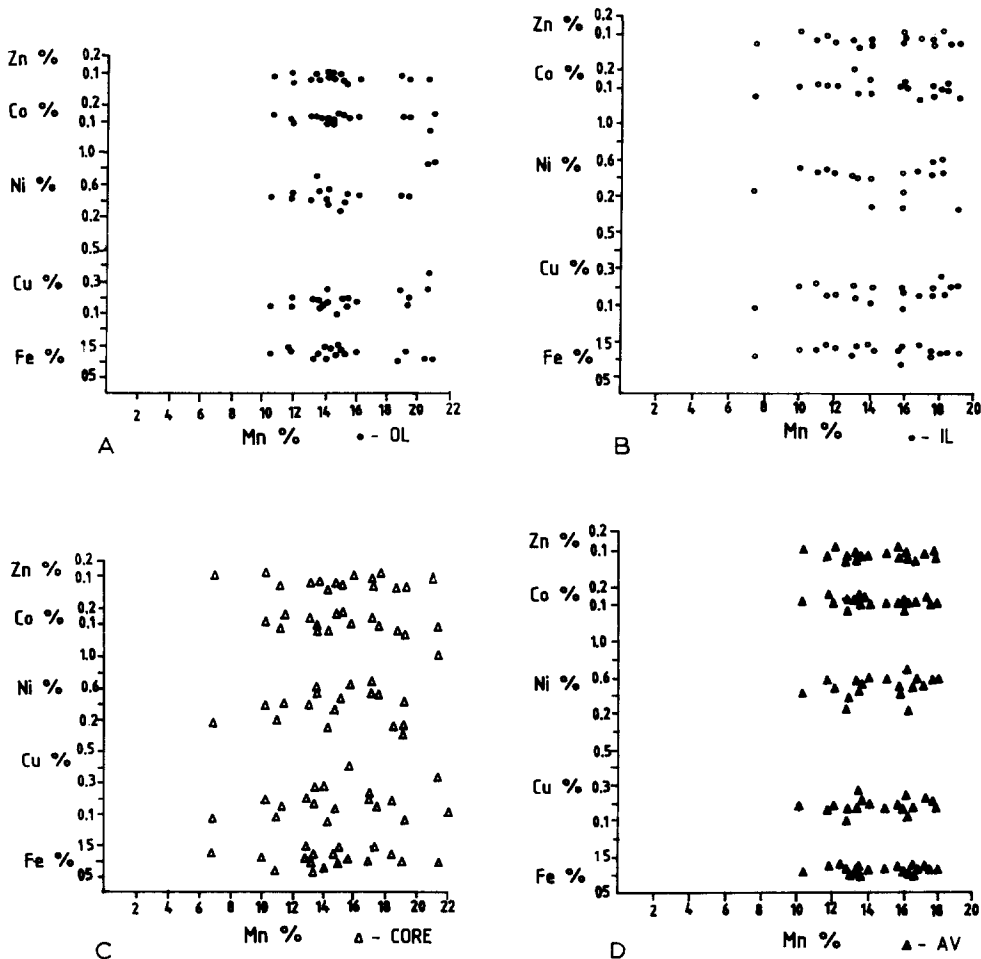


Fig.5.A–D. Variation of Fe, Cu, Ni, Co and Zn with Mn for the OL, IL, Core and the average.

TABLE 3

Average chemical composition of manganese nodules from the Carlsberg Ridge

Serial No.	Station No.	Mn (%)	Fe (%)	Ni (%)	Cu (%)	Co (%)	Zn (%)	Mn/Fe	Cu/Ni	Ni + Cu (%)	Ni + Cu + Co (%)
1	1902	12.75	11.77	0.29	0.10	0.09	0.05	1.13	0.34	0.39	0.48
2	1907/1	13.33	10.80	0.43	0.17	0.29	0.09	1.28	0.67	0.60	0.86
3	1908/3	11.66	12.93	0.56	0.17	0.15	0.08	0.90	0.30	0.73	0.88
4	1925	17.19	11.62	0.52	0.23	0.14	0.08	1.48	0.44	0.75	0.89
5	1932/2	15.75	12.27	0.43	0.17	0.16	0.08	1.28	0.40	0.60	0.76
6	1933	14.26	13.64	0.53	0.21	0.12	0.10	1.20	0.40	0.80	0.86
7	1934	15.38	13.00	0.47	0.18	0.13	0.11	1.18	0.38	0.65	0.77
8	1935/1	16.25	11.67	0.23	0.12	0.12	0.09	1.39	0.52	0.35	0.47
9	1935/2	16.51	11.52	0.57	0.18	0.12	0.07	1.43	0.32	0.75	0.87

TABLE 4

Average chemical composition of nodules reported from the Carlsberg Ridge and Indian Ocean

Reference	Area	Mn (%)	Fe (%)	Ni (%)	Cu (%)	Co (%)	Zn (%)	Mn/Fe	Cu/Ni	Ni + Cu (%)	Ni + Cu + Co (%)
1	CR Av	14.79	12.14	0.45	0.17	0.15	0.08	1.25	0.38	0.62	0.76
2	CR Av	16.46	14.62	0.51	0.13	0.27	-	1.13	0.25	0.64	0.91
3	CR Av	16.40	16.90	0.57	0.26	0.15	0.06	0.97	0.46	0.83	0.98
4	Ind Av	15.40	14.80	0.46	0.27	0.22	0.07	1.04	0.59	0.73	0.95
5	Ind Av	15.42	15.74	0.40	0.16	0.30	-	1.03	-	0.56	0.86

1 = This paper; 3 and 4 = Cronan and Moorby (1981); 2 and 5 = S.I.O (1982); CR Av — Carlsberg Ridge average; Ind Av — Indian Ocean average.

TABLE 5

Average chemical composition of different types of nodules from dredge station 1933

Sample No.	Nodule type	Mn (%)	Fe (%)	Ni (%)	Cu (%)	Co (%)	Zn (%)	Ni + Cu + Co (%)	Mn/Fe
1	SPs	13.42	13.87	0.45	0.19	0.12	0.05	0.76	0.97
2	SPr	17.87	11.57	0.59	0.19	0.12	0.08	0.90	1.54
3	DPs	16.08	11.97	0.68	0.24	0.10	0.09	1.02	1.34
4	DPs	14.08	11.80	0.58	0.20	0.13	0.08	0.91	1.19
5	Ss	13.63	9.15	0.52	0.21	0.12	0.09	0.85	1.49
6	SPr	13.33	11.67	0.56	0.28	0.13	0.09	0.97	1.14
7	SPs	17.63	12.80	0.58	0.22	0.11	0.14	0.91	1.38
8	Sr	12.00	12.60	0.41	0.17	0.11	0.12	0.69	0.95
9	Sr	10.34	13.70	0.42	0.18	0.11	0.12	0.71	0.79

For explanation of abbreviations, see Table 1.

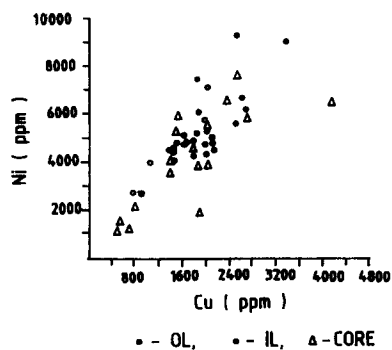


Fig.6. Variation of Ni with Cu.

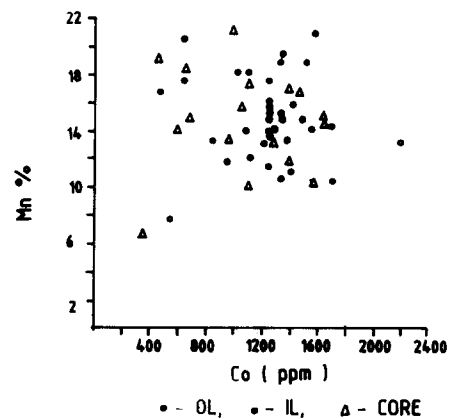


Fig.8. Variation of Mn with Co.

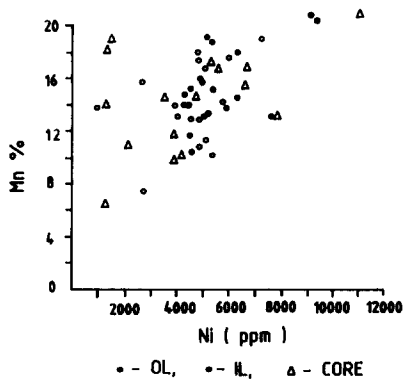


Fig.7. Variation of Mn with Ni.

Ni shows a positive correlation with Mn (Fig.7). Colley et al. (1979) observed in ridge samples that Cu shows a positive correlation and Ni a negative correlation with Mn. Cobalt shows a positive correlation with Mn only in OL

samples (Fig.8). No correlation is observed between Zn and Mn, both elements behaving independently of each other (Fig.9).

The interelement relationships for the OL, IL, Core, average and whole data analyses are shown in Table 6. It can be seen that Mn correlates strongly with Ni and Cu in the OL samples and in the IL and Core samples, Mn and Ni correlation is significant. A very strong correlation is seen between Ni and Cu in all the layers analysed, and also in the averages and whole data analyses. Zinc, Ni and Cu in the Core samples show strong positive correlations. In the OL, IL and average values, Zn correlates negatively with Mn, Fe, Ni, Cu and Co. Interestingly, no significant positive correlation is observed between Co and the other elements.

TABLE 6A

Interelement relationship in Carlsberg Ridge nodules (OL).
 $N=18$; $R=0.40$ for $r=95\%$

	Mn	Fe	Ni	Cu	Co	Zn
Mn	1.00					
Fe	-	1.00				
Ni	0.52	-	1.00			
Cu	0.54	-	0.80	1.00		
Co	-	-	-	-	1.00	
Zn	-	-	-	-	-	1.00

TABLE 6B

Interelement relationship in Carlsberg Ridge nodules (IL).
 $N=18$; $R=0.40$ for $r=95\%$

	Mn	Fe	Ni	Cu	Co	Zn
Mn	1.00					
Fe	-	1.00				
Ni	0.41	-	1.00			
Cu	-	-	0.51	1.00		
Co	-	-	-	-	1.00	
Zn	-	-	-	0.40	-	1.00

TABLE 6C

Interelement relationship in Carlsberg Ridge nodules (Core). $N=17$; $R=0.41$ for $r=95\%$

	Mn	Fe	Ni	Cu	Co	Zn
Mn	1.00					
Fe	-	1.00				
Ni	0.41	-	1.00			
Cu	-	-	0.81	1.00		
Co	-	-	-	-	1.00	
Zn	-	-	0.56	0.58	-	1.00

TABLE 6D

Interelement relationship in Carlsberg Ridge nodules (average). $N=18$; $R=0.40$ for $r=95\%$

	Mn	Fe	Ni	Cu	Co	Zn
Mn	1.00					
Fe	-	1.00				
Ni	-	-	1.00			
Cu	-	-	0.80	1.00		
Co	-	-	-	-	1.00	
Zn	-	-	-	-	-	1.00

TABLE 6E

Interelement relationship in Carlsberg Ridge nodules (whole data). $N=53$; $R=0.22$ for $r=95\%$

	Mn	Fe	Ni	Cu	Co	Zn
Mn	1.00					
Fe	-	1.00				
Ni	0.43	-	1.00			
Cu	0.37	-	0.75	1.00		
Co	-	-	-	-	1.00	
Zn	-	-	0.38	0.42	-	1.00

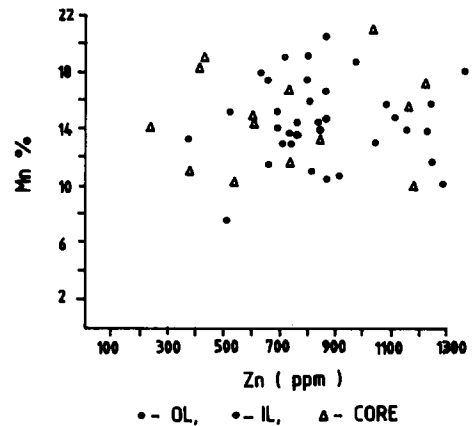


Fig.9. Variation of Mn with Zn.

Discussion

Physical parameters and abundance

Nodules of mixed facies are of considerable interest. Many investigators have correlated physical properties of nodules to their chemical composition. Heye (1979), in seamount and abyssal plain nodules from the Central Pacific, found a decrease in Fe and an increase in Mn, Ni and Cu corresponding to an increase in maximum diameter. Although such relationships cannot be generally applied to other oceans, the present study does show a similar relationship in the Carlsberg Ridge nodules. The average chemical composition (Table 3), however, does not match with that of the Central Pacific seamounts; the variation of Mn, Ni and Cu is quite large because the seamount nodules cannot be compared chemically with those of the active ridge.

The present study also indicates that rough-surface nodules are richer in Mn, Ni and Cu than smooth-surface nodules, an observation similar to that of many investigators (Meyer, 1973; Fujinuki et al., 1977; Mizuno and Moritani, 1977; Halbach and Özkara, 1979; Heye, 1979) who correlated physical properties (morphology and surface texture) with chemical composition. Rough-surface nodules, according to Raab (1972), are buried within the sediments. The growth of a buried nodule, therefore, takes place by accreting 10 Å manganates from sediment pore water enriched in Ni and Cu which subsequently become concentrated in the rough-surface nodules. The highest average value of the Mn/Fe ratio (1.48) in the Sr-type nodules is significant in this respect (Table 1).

The lowest nodule abundance (1.1 kg/m², station 1925) is associated with dominant Sr-type nodules. Rough nodules with highest values for Mn (20.75%), Ni (0.92%), Cu (0.33%) and Co (0.16%) in the OL show an inverse relationship with abundance (sample 14, Table 1). Ellipsoidal nodules with a smooth surface (Ss) texture (station 1935/2) (abundance of 3.03 kg/m²) have the highest concentration of Mn (19.0%) and Ni (0.73%) in the IL and the highest concentration of Co (0.17%) in the Core samples 68 and 70, Table 1). The greatest abundance (5.85 kg/m²) was recorded at station 1907/1 where the Co concentration is highest in the Core (0.68%) (sample 8, Table 1).

An inverse correlation between abundance and nodule grade has been reported in Pacific Ocean nodules. The major factors affecting this relationship, according to Frazer and Fisk (1981), are sediment type and local topography. Mizuno and Moritani (1977) noted a similar inverse correlation in the nodules associated with siliceous clay. In contrast, smooth-surface nodules associated with clays are lower in Mn, Ni and Cu.

Mineralogy

Colley et al. (1979) reported enrichment of Ni and Cu in nodules from the Carlsberg Ridge

and noted significantly low levels of Co, an observation confirmed in the present study. The todorokite-rich samples normally contain higher Cu + Ni (0.66%) and Mn/Fe (1.65) levels, whereas samples rich in δ -MnO₂ will contain lower Cu/Ni levels (up to 0.30%) and lower Mn/Fe levels (0.48–0.74). Such low values of Cu/Ni were obtained only at one station 1908/3 (Table 3).

Karisiddaiah (1985) observed an association of alternate layers of δ -MnO₂ and FeOOH·XH₂O in our nodules and suggested hydrogenesis involving slow precipitation of hydrated metal oxides from near-bottom seawater as the cause. According to Halbach et al. (1982), the formation of todorokite depends on the supply of Mn²⁺ ions during early diagenetic conditions in the pore water. Burns and Burns (1978) suggested post-recrystallisation processes leading to the formation of authigenic todorokite in the nodules. Similar processes must be responsible for the formation of todorokite platelets in the Carlsberg Ridge nodules. Veinlets of todorokite within the nucleus of Pacific Ocean nodules were also reported by Chukrov et al. (1979).

Genesis

In order to discuss the genesis of the Carlsberg Ridge nodules, the Bonatti et al. (1972) diagram (Fig.10) has been used. Ninety-three percent of the samples occupy the central

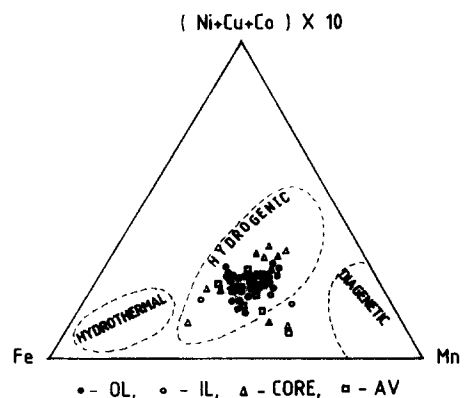


Fig.10. Fe-Mn-(Ni + Cu + Co) × 10 diagram.

field of hydrogenous Pacific Ocean nodules. The remaining samples are close to this field. Hydrogenous deposits are normally formed by slow precipitation of Mn and Fe from seawater. The presence of the δ -MnO₂ mineral phase in all the samples suggests that nodule formation took place under high degrees of oxidation.

The strong correlation observed between Cu and Ni indicates that these elements were available in Mn oxide phases. Correlation of Mn with Ni and Cu in the OL and whole data analyses also supports this interpretation. However, the absence of a correlation between Mn and Cu in the IL suggests an intermittent supply of Cu during nodule growth.

A nodule can grow by receiving metals from both seawater and interstitial water and a mixing model for this process has been suggested by Piper and Williamson (1981). Their interpretation was that the differences in the thermodynamic properties of Fe and Mn were responsible for the high Mn/Fe ratios of 35:1 in the outermost bottom layer and of between 1:1 and 2:1 in the near-surface layers of the nodules. In the present case, the Mn/Fe ratio ranges between 0.54 and 2.28 which indicates that in these nodules the major contribution of metal is from seawater. Variations in the interlayer and bulk compositions are due to variation in the source of supply which indicates different rates of accretion for different nodule layers.

Conclusions

Analysis of the seven different types of manganese nodules recovered from the Carlsberg Ridge has led to the following conclusions:

(1) The concentrations of Mn, Cu and Co are related to nodule diameter.

(2) Rough-surface spheroidal and ellipsoidal nodules (Sr-type) show a gradual increase in Mn, Fe, Ni, Cu, Co and Zn from the Core to the OL, while smooth-surface irregular, elongated and flattened types (ISs) and flattened types (DPs) show decreasing concentrations of these

elements. Further, the Sr-type nodules contain the highest concentrations of Mn, Ni, Cu, Co and Zn in the OL.

(3) Sr-type nodules are the most abundant, whereas Ss-type nodules are the least abundant.

(4) δ -MnO₂ is the dominant mineral phase and the nodule mineralogy suggests formation under hydrogenetic and diagenetic conditions, the nodule composition in particular suggesting fractionation of Cu and Ni by hydrogenetic processes. Finally, the layerwise chemical variation is due to variation in the source of metal supply.

Acknowledgements

The authors are grateful to Dr. S.Z. Qasim, secretary of the D.O.D. and former director of the N.I.O. for his constant encouragement. Thanks are also due to the master, crew and all other participants of the 86th and 87th cruises of the R.V. *Gaveshani* who helped during sample collection. We are extremely grateful to an anonymous reviewer for suggestions for improvements in the manuscript. Help rendered by Shri V.M. Date, A. Sheikh and by Shri S. Akerkar in the preparation of the figures is also gratefully acknowledged.

References

- Bonatti, E., Kraemer, T. and Rydell, H., 1972. Classification and genesis of submarine iron-manganese deposits. In: D.R. Horn (Editor), *Ferromanganese Deposits on the Ocean Floor*. Natl. Sci. Found., Washington, D.C., pp.149-166.
- Burns, V.M. and Burns, R.G., 1978. Post-depositional metal enrichment processes inside manganese nodules from the north equatorial Pacific. *Earth Planet. Sci. Lett.*, 39: 341-348.
- Chukrov, F.V., Gorshkov, A.I., Sivstov, A.V. and Beresovskaya, V.V., 1979. New data on natural todorokite. *Nature*, 278: 631-632.
- Colley, N.M., Cronan, D.S. and Moorby, S.A., 1979. Some geochemical and mineralogical studies on newly collected ferromanganese oxide deposits from the north-west Indian Ocean. In: C. Lalou (Editor), *La Genèse des Nodules de Manganèse*. Colloq. Int. C.N.R.S., 289: 13-21.
- Cronan, D.S., 1967. Geochemistry of some manganese nodules and associated pelagic deposits from the Pacific

- and Indian Oceans. Ph.D. Thesis, Univ. London, London (Unpubl.).
- Cronan, D.S. and Moorby, S.A., 1981. Manganese nodules and other ferromanganese oxide deposits from the Indian Ocean. *J. Geol. Soc. London*, 138: 527-539.
- Cronan, D.S. and Tooms, J.S., 1968. A microscopic and electron probe investigation of manganese nodules from the northwest Indian Ocean. *Deep-Sea Res.*, 15: 215-223.
- Dunham, A.C. and Glasby, G.P., 1974. Petrographic and electron microprobe investigation of some deep- and shallow-water manganese nodules. *N.Z. J. Geol. Geophys.*, 17(4): 929-953.
- Frazer, J.Z. and Fisk, M.B., 1981. Geological factors related to characteristics of sea-floor manganese nodule deposits. *Deep-Sea Res.*, 28(A12): 1533-1551.
- Fujinuki, T., Mochizuki, T. and Moritani, T., 1977. Chemical composition of manganese nodules. In: A. Mizuno and T. Moritani (Editors), *Deep Sea Mineral Resources Investigation in the Central-Eastern part of the Central Pacific Basin, Jan.-Mar., 1976 (GH 76-I cruise)*. *Geol. Surv. Jpn., Cruise Rep. No. 8*, pp.162-171.
- Glasby, G.P., 1970. The geochemistry of manganese nodules and associated pelagic sediments from the Indian Ocean. Ph.D. Thesis, Univ. London, London (Unpubl.).
- Glasby, G.P., 1972. The geochemistry of manganese nodules from the Northwest Indian Ocean. In: D.R. Horn (Editor), *Ferromanganese Deposits on the Ocean Floor*. *Natl. Sci. Found., Washington, D.C.*, pp.93-104.
- Glasby, G.P., 1973. Distribution of manganese nodules and lebensspuren in under water photographs from the Carlsberg Ridge, Indian Ocean. *N.Z.J. Geol. Geophys.*, 16: 1-17.
- Halbach, P. and Özkara, M., 1979. Morphological and geochemical classification of deep-sea ferromanganese nodules and its genetical interpretation. In: C. Lalou (Editor), *La Genèse des Nodules de Manganèse. Colloq. Int. C.N.R.S.*, 289: 77-88.
- Halbach, P., Giovanoli, R. and Von Borstel, D., 1982. Geochemical processes controlling the relationship between Co, Mn and Fe in early diagenetic deep sea nodules. *Earth Planet. Sci. Lett.*, 60: 226-236.
- Heye, D., 1979. Relationship between the size of manganese nodules in the Central Pacific, their chemical constitution and other parameters. In: C. Lalou (Editor), *La Genèse des Nodules de Manganèse. Colloq. Int. C.N.R.S.*, 289: 89-91.
- Karisiddaiah, S.M., 1985. Mineralogy and chemistry of manganese nodules from the southern part of Carlsberg Ridge. *J. Geol. Soc. India*, 26: 402-406.
- Meyer, K., 1973. Surface sediment and manganese nodule facies encountered on R/V Valdivia cruises 1971/3. In: M. Morgenstein (Editor), *Papers on the Origin and Distribution of Manganese Nodules in the Pacific and Prospects for Exploration*. *Hawaii Inst. Geophys., Honolulu*, pp.125-130.
- Mizuno, A. and Moritani, T., 1977. Outline of GH 76-I cruise and its results. In: A. Mizuno and T. Moritani (Editors), *Deep Sea Mineral Resources Investigation in the Central-Eastern Part of the Central Pacific Basin, Jan.-Mar., 1976 (GH 76-I Cruise)*. *Geol. Surv. Jpn., Cruise Rep. No. 8*, p.20.
- Moritani, T., Maruyama, S., Nohara, M., Matsumoto, K., Ogitsu, T. and Moriwaki, H., 1977. Description, classification and distribution of manganese nodules. In: A. Mizuno and T. Moritani (Editors), *Deep Sea Mineral Resources Investigation in the Central-Eastern Part of the Central Pacific Basin*. *Geol. Surv. Jpn., Cruise Rep. No. 8*, pp.136-158.
- Piper, D.Z. and Williamson, M.E., 1981. Mineralogy and composition of concentric layers within a manganese nodule from the north Pacific. *Mar. Geol.*, 40(3/4): 255-268.
- Raab, W., 1972. Physical and chemical features of Pacific deep sea manganese nodules and their implications to the genesis of nodules. In: D.R. Horn (Editor), *Ferromanganese Deposits on the Ocean Floor*. *Natl. Sci. Found., Washington, D.C.*, pp. 31-50.
- Scripps Institute of Oceanography (S.I.O.), 1982. Data storage bank.